Synapse

WILEY

SYNAPSE

RESEARCH ARTICLE OPEN ACCESS

Increased Expression of Synaptic Vesicle Glycoprotein 2A (SV2A) in the Brain of Chronic Diabetic Rats

Burcu Azak Pazarlar[1,2,3] | Cansu Bilister Egilmez[3] | Eser Öz Oyar[3] | Jens D. Mikkelsen[1,2]

[1]Department of Neuroscience, University of Copenhagen, Copenhagen, Denmark | [2]Neurobiology Research Unit, University Hospital Copenhagen, Rigshospitalet, Copenhagen, Denmark | [3]Physiology Department, Faculty of Medicine, Izmir Katip Celebi University, Izmir, Turkey

Correspondence: Burcu Azak Pazarlar (burcu.pazarlar@sund.ku.dk)

Received: 31 January 2025 | **Revised:** 14 April 2025 | **Accepted:** 16 April 2025

Funding: The project was funded by Izmir Katip Celebi University Scientific Research Project Council with project number 2014-ÖNP-TIPF-0028 to BAP and EOO and the NOVO Nordisk Foundation Tandem Grant (#NNF23OC0081536) to JDM.

Keywords: diabetes | glutamate | hyperglycemia | rat | SV2A | synapse

ABSTRACT

Aim/hypothesis: Diabetes mellitus has been reported to be a risk factor for cognitive dysfunction, depression, stroke, and seizures. Diabetic pathology is believed to interfere with synaptic plasticity. Synaptic vesicle glycoprotein 2A (SV2A) is a presynaptic vesicular protein and a popular synaptic density imaging marker. We investigated the effect of chronic hyperglycemia on the expression of SV2A in the cerebral cortex and hippocampus of rats and compared it to other presynaptic markers, such as GAP43, Synaptotagmin-1, and SNAP25.

Methods: A single dose of streptozotocin (STZ, 45 mg/kg, i.p.) was administered to adult male rats, resulting in sustained hyperglycemia and reduced plasma insulin levels. Controls were injected with saline, and another STZ group was treated with insulin. Fasting blood glucose (FBG) and fasting plasma insulin (FPI) levels were monitored throughout the observation period, and the level of SV2A was determined by radioligand, [^{3}H]UCB-J, binding capacity using in-vitro autoradiography and by ELISA. Similarly, the tissue concentration of other synaptic proteins GAP43, SNAP25, and SYN1 was measured using ELISA. Quantitative RT-qPCR was performed to measure *Sv2a, Sv2b*, and *Sv2c* transcripts. Finally, hippocampal and cortical glutamate levels were measured in all tissues.

Results: [^{3}H]UCB-J binding, SV2A (pg/mg protein) and *Sv2a* mRNA levels were significantly higher in hyperglycemic rats. The SV2A concentration detected by ELISA and [^{3}H]UCB-J binding showed, as expected, a positive correlation with each other. The same positive and significant correlation was seen between SV2A, FBG, and glutamate l levels across animals ($p \leq 0.001$). Notably, there was no difference and no linearity between FBG and other presynaptic markers such as GAP43, Synaptotagmin-1, and SNAP25.

Conclusions: Unlike other synaptic markers (e.g., SNAP25, SYN-1), SV2A levels rise independently of synaptic density, correlating with elevated glutamate and metabolic activity. These findings raise doubt about SV2A's role as a pure synaptic density marker.

1 | Introduction

Type I diabetes mellitus is a chronic metabolic disorder characterized by hyperglycemia caused by insulin deficiency (Acharjee et al. 2013; Bluestone et al. 2010). Type I diabetes patients have a higher prevalence of cognitive decline (Broadley et al. 2017; Ding et al. 2019), depression (Bădescu et al. 2016; Pan et al. 2010), and seizure susceptibility (Hiremath et al. 2019; Stafstrom 2003).

In experimental studies, changes in brain tissue volume and cerebral blood flow (Last et al. 2007), conductance of nerve fibers (Nissen et al. 2020); increase in firing frequency of neurons (Roberts et al. 2017) and synaptic loss (Zhao et al. 2016) were shown in diabetic patients. Peripheral insulin levels have been proposed to affect neuroplasticity (Grillo et al. 2019), and hyperglycemia is thought to impact neurogenesis negatively (Dorsemans et al. 2017). Experimental studies in animals have further revealed that diabetes leads to changes in both synaptic spine number and structure in cortical neurons (Joghataie et al. 2007; Martínez-Tellez et al. 2005) and in the spinal cord (Tan et al. 2012). Aligned with these observations, animal models of type II diabetes induced by a high-fat diet or genetically have also shown abnormal hippocampal neuroplasticity as well as learning and memory deficits (Grillo et al. 2019).

Glutamatergic neurotransmission is key for long-term potentiation plasticity and changes in hippocampal synapses (Bliss and Collingridge 2013). Because glutamate is increased in diabetic patients' brains (Fried et al. 2019; Wiegers et al. 2019), the increase in glutamate neurotransmission is likely involved in synaptic plasticity in the diabetic brain (Bolo et al. 2020; d'Almeida et al. 2020; Fried et al. 2019; Terpstra et al. 2014; Wiegers et al. 2019).

Synaptic vesicle glycoprotein 2A (SV2A) is a presynaptic vesicle membrane protein and a member of the SV2 protein family that also includes SV2B and SV2C (Bajjalieh et al. 1993). Loss-of-function studies have shown that SV2A is important in regulating neurotransmitter release in vitro (Janz et al. 1999; Lynch et al. 2004; Menten-Dedoyart et al. 2016). The expression pattern of SV2 transcripts in the human cerebral cortex is distributed in a cell type-specific manner, with SV2A expressed in all glutamatergic and GABAergic neuronal subtypes, whereas SV2B is only expressed in the glutamatergic neurons (Pazarlar et al. 2022).

In addition, SV2A has been considered a marker of synaptic density (Carson et al. 2022). To investigate the effects of high glucose levels on synaptic density, we utilized the specific radioligand, [^{3}H]UCB-J, to assess its binding to SV2A as a proxy measure of synapse density in a type 1 diabetic animal model. We additionally employed immunodetection of SV2A in the same brains and tissues. To relate any changes in SV2A to synaptic plasticity, we also expanded our examination to other established synaptic proteins, including growth-associated protein-43 (GAP43), synaptosome-associated protein 25 (SNAP25), and synaptotagmin 1 (SYN-1) in the same tissue samples used for SV2A measurements. As SV2A levels seemed to fluctuate independently of the other synaptic markers, we became intrigued by any factors that may regulate SV2A levels. For this purpose, we correlated SV2A levels with either blood glucose or brain glutamate, both known to be changing in experimental diabetes and under hyperglycemic conditions (Fried et al. 2019; Wiegers et al. 2019).

2 | Materials and Methods

2.1 | Animals, Treatments, and Tissue Sampling

Sprague–Dawley rats used in these experiments were bred and housed under room temperature, humidity (55 ± 5%), and 12 h light/dark cycle in Celal Bayar University Laboratory Animals Research Center. After weaning, 4 rats per cage were kept with free access to tap water and a normal chow basal diet. Approximately 3-month-old male rats weighing 300–350 g were included in the experiment and randomly divided into three groups as shown in Figure 1A. In this study, we chose to use male rats to minimize potential variability related to hormonal fluctuations of female rats that might affect the outcomes (Rocha et al. 2022). Additionally, no sex-specific differences related to SV2A level were anticipated based on existing literature (Michiels et al. 2021).

Group 1 (Control) (n = 6) was given a single intraperitoneal (i.p.) dose of 300 µL fresh citrate buffer (0.1 M; pH 4.5). Group 2 (diabetic, Db) (n = 13) was given a single injection with 45 mg/kg i.p. streptozotocin (STZ, Sigma Chemical Co., St Louis, MO, USA) dissolved in citrate (Furman 2015) after fasting for 12 h. Fasting blood glucose (FBG) (mmol/L) levels were measured from the tail vein blood to confirm the hyperglycemia (Accu-Check, Roche, Germany), and concentrations higher than 13.9 mmol/L 72 h after the STZ injection were considered diabetic (inclusion criteria) (Michiels et al. 2021). Group 3 (insulin-treated group, Ins) (n = 13) was given glargine-type long-acting insulin (Lantus, Sanofi) with a dose of 5 units/kg/day (Deeds et al. 2011) subcutaneously and daily for 8 weeks after the STZ injection. All animals were kept in their cages with free access to food and water during the observation period.

Body weights, FBG, and fasting plasma insulin (FPI) were monitored weekly. Blood samples were collected in tubes containing EDTA and centrifuged at 2500 × g for 15 min at 4°C, and plasma was stored at -80°C until analysis. Plasma insulin levels were measured by a commercial kit (RAB0904, Sigma-Aldrich) according to the manufacturer's instructions.

At the 8-week time point, the animals were decapitated under sodium pentobarbital (i.p. 80 mg/kg) anesthesia, and the brains were rapidly removed. One-half of the hemispheres (left) were dissected to isolate the cerebral cortex and hippocampus, which were then used for transcript and protein expression analysis. The remaining half of the hemisphere and brainstem (right) was frozen intact within powdered dry ice and utilized for the radioligand binding analysis. All tissues were stored at –80°C until analysis.

2.2 | Autoradiography Procedure

Serial sagittal brain sections, each 20 µm thick and located approximately 2.4 mm lateral to bregma, were cut using a cryostat and mounted onto Superfrost Plus glass slides (Thermo Fisher Scientific), with three sections per slide. The experimental groups included 6 control animals, 7 diabetic (Db) animals, and 7 insulin-treated (Ins) animals. To minimize inter-assay variability, all slides were processed concurrently.

Pre-incubation of the slides was performed twice for 10 min at room temperature in a 50 mM Tris-HCl buffer (pH 7.4) containing 0.5% bovine serum albumin (BSA; Sigma, Cat. No. A9647). Subsequent incubation lasted 60 min in the same buffer, supplemented with 5 mM $MgCl_2$, 2 mM EGTA, and 6 nM [^{3}H]UCB-J. The radioligand [^{3}H]UCB-J ((R)-1-((3-pyridin-4-yl)

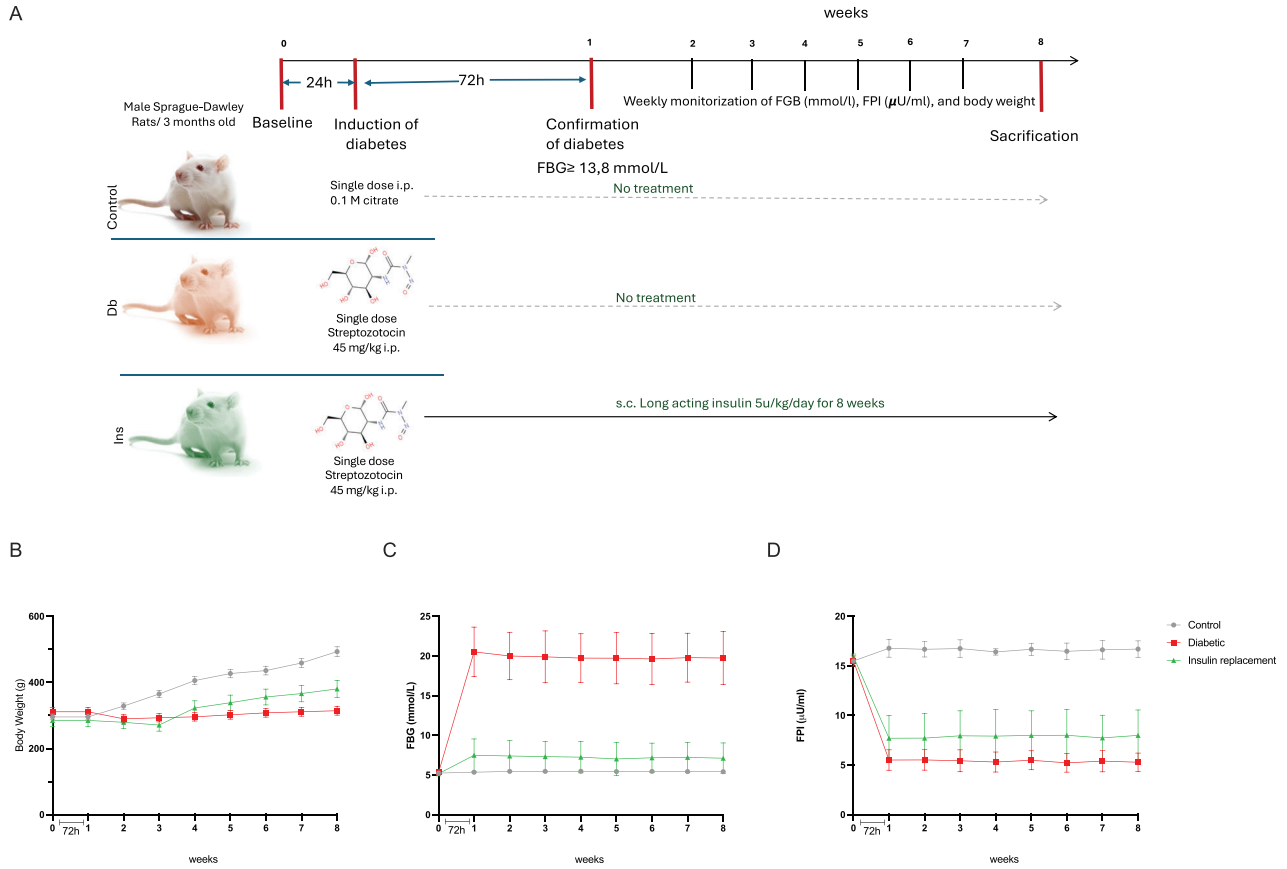

FIGURE 1 | Experimental design and biochemical measures during 8 weeks.
Experimental timeline and treatments for each group were schematized. (A) Body weight is shown that was monitored weekly. (B) The follow-up for 8 weeks for fasting blood glucose (FBG mmol/L) (C) and fasting plasma insulin (FPI, μU/mL) (D) were also shown. There is a statistical increase in FBG values of the diabetic group (red line) compared to control (gray line) starting from the first and that increase was sustained for 8 weeks ($p < 0.0001$; ****). The increase was kept under control in insulin-treated group with slightly higher levels than the control ($p < 0.01$; **). On the contrary, FPI levels significantly decreased in the diabetic group ($p < 0.0001$; ****) but the decrease was less pronounced in insulin-treated group ($p < 0.0001$; ****). Repeated measures component was included to analyze longitudinal data. Values are given as mean ± SD.

methyl)-4-(3,4,5-trifluorophenyl)pyrrolidin-2-one; TRQ41493) was synthesized by UCB Pharma (Braine l'Alleud, Belgium) and radiolabeled by Quotient Bioresearch Ltd. (UK), with a specific activity of 24 Ci/mmol at synthesis. The radiochemical concentration was 1 mCi/mL on the day of synthesis, and specific activity was verified on the day of the experiment.

After incubation, sections underwent two 10-min washes at 4°C in ligand-free buffer, followed by a brief rinse in distilled water. The slides were then fixed overnight in a paraformaldehyde vapor chamber and dried under airflow. For autoradiography, the slides were exposed to FUJI imaging plates at 4°C for three days, alongside [^{3}H] standards that covers the data range for this experiment (ARC, American Radiolabeled Chemicals, Inc., USA; and [^{3}H] microscale Batch 21A, GE Healthcare, UK). Imaging plates were scanned using a Fujifilm Image Reader (BAS-2500 V1.8), and autoradiograms were analyzed with ImageJ software (Version 2.0.0, NIH).

Regions of interest (ROIs), including the cerebral cortex, hippocampus, thalamus, and brainstem, were delineated based on a rat brain atlas to ensure consistent measurement areas across sections. The corpus callosum, representing the largest white matter region, served as a reference for non-specific binding within the same section. Because the [^{3}H]UCB-J binding in white matter is negligible, as demonstrated in our previous study (Deeds et al. 2011), based on the lack of synapses. This in vitro approach is also consistent with established in vivo clinical [^{11}C]UCBJ imaging practices (Rossano et al. 2020). Accordingly, ROI measurements were adjusted by subtracting corpus callosum values. Optical density readings in ROIs were interpolated from known [^{3}H] standards (nCi/mg) and converted to femtomoles of bound radioligand per milligram of tissue equivalent (fmol/mg TE). Image analyses were conducted by two researchers, one of whom was blinded to the experimental conditions to mitigate potential bias.

2.3 | Determination of Presynaptic Proteins With ELISA

Frozen cerebral cortex and hippocampus tissues from control ($n = 6$), diabetic ($n = 13$), and insulin-treated ($n = 13$) rats were homogenized in a lysis buffer (150 mM NaCl, 1% Triton

X-100, and 10 mM Tris, pH 7.4) containing a protease inhibitor (Abcam, ab271306). The homogenate was centrifuged at 10,000 × *g* for 10 min at 4°C and the supernatant was collected for the determination of total protein levels using the Pierce BCA Protein Assay Kit (Thermo Fischer, Cat. No. # 23227). Commercial ELISA kits for SV2A (Abbexa, US, #abx548001), SNAP25 (Abcam, ab256394), GAP43 (Abbexa, US, abx354228), and SYN1 (Abbexa, US, abx391308) were used, and the immunoreactivities were colorimetrically determined according to the instructions of the manufacturers. Standard curves were generated with known concentrations of standard sample proteins, and the samples were diluted until the optical density (OD) values fell within the best range for detection. Total protein levels were determined in all extracts and expressed as pg/mg protein.

2.4 | Glutamate Measurements

Glutamate levels were determined by using a commercial kit (#ab83389, glutamate assay kit, Abcam, UK). Briefly, the same homogenates that were used for protein measurements from control ($n = 6$), diabetic ($n = 13$), and insulin-treated ($n = 13$) rats were used and centrifuged at 15,000 × *g* for 5 min, and the supernatant was collected for the determination of glutamate concentrations. The standards and samples were prepared according to the manufacturer's instructions. The final absorbance was read at 405 nm in a UV-VIS spectrophotometer (Jasco, Model 760) and the levels were presented as nmol/mg protein.

2.5 | Gene Expression Analysis With Quantitative Real-Time PCR

Total RNA was extracted from the homogenates of frozen cerebral cortex and hippocampus tissues from control ($n = 6$), diabetic (Db, $n = 13$), and insulin-treated (Ins, $n = 13$) rats using the Quick-RNA MiniPrep Kit (Zymo Research, Cat. No. R10564). The RNA yield and purity were assessed by measuring UV absorbance at 260 nm and 280 nm using a Nanodrop microvolume spectrophotometer (Thermo Fisher Scientific, 2000/2000c). RNA samples with appropriate A260/A280 ratios were selected for subsequent analyses. Reverse transcription of the purified RNA into complementary DNA (cDNA) was performed using the Promega reverse transcription system (Cat. No. A3800) and a BioRad iCycler Thermal Cycler. The reaction mixture (20 μL total volume) consisted of 4 μL 5× Improm-II buffer, 4.8 μL $MgCl_2$, 1 μL dNTP mix, 0.5 μL recombinant RNasin ribonuclease inhibitor, 1 μL oligo(dT) primers, and 7.7 μL RNA. Reverse transcription conditions included an initial step at 25°C for 5 min, followed by incubation at 42°C for 60 min, and a final extension at 72°C for 15 min.

Quantitative PCR (qPCR) was performed using the BioRad iQ SYBR Green Supermix (Cat. No. 170–8880) on a Roche LightCycler 480 II instrument. Each 20 μL reaction contained 11 μL SYBR Green mix, 5 μL cDNA template, 15 pmol of forward primer, 15 pmol of reverse primer, and nuclease-free water. Amplification was carried out in a 96-well plate with the following thermal cycling parameters: an initial denaturation step at 95°C for 3 min, followed by 40 cycles of 95°C for 15 s, 60°C for 30 s, and 72°C for 30 s. After amplification, a melting curve analysis was performed to verify primer specificity.

Primers for target genes Sv2a, Sv2b, and Sv2c were designed using NCBI's Primer-BLAST tool and verified experimentally for specificity and efficiency through test amplifications. The following primer sequences were used: Sv2a (NM_057210): F: 5′-TCTCTGCTCCAGGTGTTCCA-3′, R: 5′-GGAGGCTAAGGTTTATTGCTAC-3′. Sv2b (NM_057207.3): F: 5′-CTAAGCAGACTAAGATGGCAC-3′, R: 5′-TCTGGCATGAACTTCAGGGCCAC-3′. Sv2c (NM_031593.1): F: 5′-ATCAAGACTCCCAAGCAAATAG-3′, R: 5′-GACAGGGTGAACCAAACAATC-3′. Gapdh (NM_017008.4): F: 5′-AAGTTCAACGGCACAGTCAAG-3′, R: 5′-CCAGTAGACTCCACGACATACTCA-3′.

We calculated relative gene expression levels using the Pfaffl method (Pfaffl et al. 2001), normalizing all target gene expression values to the reference housekeeping gene Gapdh. We included technical triplicates for all samples to ensure reliability and used appropriate controls without reverse transcriptase or template to confirm the absence of contamination.

2.6 | Statistical Analysis

Data sets were tested for normality. The data from experimental groups were analyzed using one-way ANOVA was followed by Sidak's multiple comparisons tests. Unpaired Student's *t*-test and Mann–Whitney *U* tests were used for pairwise comparisons based on the results of the Shapiro–Wilk normality test. Also, correlation analysis was performed for some data sets by using Pearson's correlation coefficient within groups and a corrected 95% confidence interval. The statistical calculations were performed using GraphPad Prism version 10 for Windows (GraphPad Software, San Diego, CA). All data were presented as a mean ± standard deviation (SD), and *p*-values of less than 0.05 were considered statistically significant.

3 | Results

3.1 | Metabolic Status of the Animals

Body weight measurements showed a 67 % increase in the control group over the 8-week observation period, but only a 1% increase in the STZ-treated diabetic group (Figure 1B). The insulin-treated group showed a moderate (30%) increase in their body weight over the 8 weeks, mostly increasing during the last 4 weeks of the observation period. After 8 weeks, body weight differed between the control and diabetic groups (Figure 1B). We monitored FBG and FPI levels weekly, beginning 3 days after the STZ injection. The final measurement was taken on the day of brain dissection. All STZ-treated rats exhibited a rapid increase in FBG levels by day 3, confirming the onset of diabetes, and hyperglycemia was sustained throughout the 8-week period, as previously described (Okamoto et al. 2011). The average FBG concentration over the 8-week observation period was 5.4 ± 0.18 mM in the control group. In contrast, the diabetic group had significantly higher FBG levels, with a mean of 19.9 ± 3.1 mM ($p < 0.0001$). The insulin-treated group showed a significant reduction in FBG compared to the diabetic group, with a mean of 7.3 ± 1.9 mM ($p < 0.01$) (Figure 1C)

The average FPI levels over the 8-week follow-up were 16.6 ± 0.71 μU/mL in the control group. The diabetic group showed

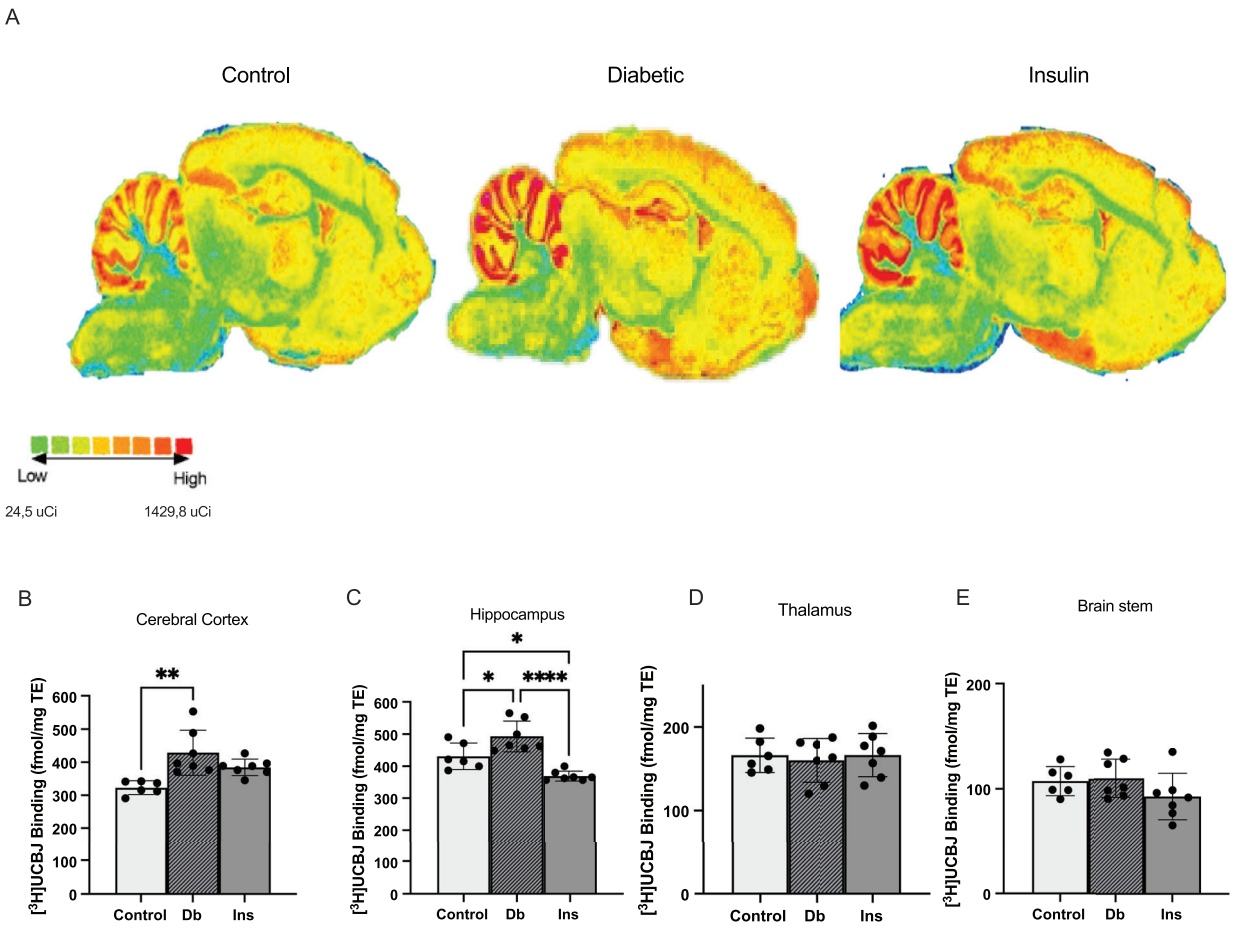

FIGURE 2 | [^{3}H]UCB-J binding levels are increased in the brain in diabetic animals.
Representative autoradiograms showing binding density in sagittal sections of the brains from control, diabetic (Db), and insulin-treated rats (Ins) (A). Most extensive labeling is observed in regions known to be dense in synapses such as the cerebral cortex, hippocampus, and cerebellum. Semi-quantitative standard-corrected measurements of binding intensities are shown as bar graphs and expressed as fmol/mg tissue equivalent (TE), for the cerebral cortex (B), hippocampus (C), thalamus (D), and brain stem (E). The level of SV2A binding is significantly higher in diabetic versus control in the cerebral cortex ($p < 0.01$) and in the hippocampus ($p < 0.05$), whereas no significant difference is seen in the thalamus and brain stem. In diabetic animals treated with insulin, the values were lower than in diabetics and reached high significance in the hippocampus but not the cerebral cortex. Comparisons were between groups performed between the control, diabetic, and insulin-treated groups for each region by one-way ANOVA test. (*$p < 0.05$, **$p < 0.01$, **** $p < 0.0001$).

significantly lower FPI levels, with a mean of 5.4 ± 0.93 μU/mL (Db vs ctrl, $p < 0.0001$). In the insulin-treated group, FPI levels were significantly lower than the control group (7.87 ± 2.47 μU/mL, $p < 0.0001$) but higher than those in the diabetic group ($p < 0.01$) (Figure 1D).

3.2 | [3H]UCB-J Binding Levels in the Brain

The in vitro autoradiography images demonstrated the distribution of bound radiotracer to sagittal sections of rat brains (Figure 2A). The binding of [^{3}H]UCB-J was accumulated in the gray matter throughout the brain. Binding was more prominent in regions with high synapse density, such as the cornu ammonia of the hippocampus and the granular cell layer of the cerebellum, while areas like the brainstem showed less intense labeling (Figure 2A). As expected, labeling in the white matter was negligible and showed no difference between the three experimental groups (not shown).

The average binding level of [^{3}H]UCB-J in the cerebral cortex of diabetic rats, was estimated to be approximately 32.6% higher (428.5 ± 68.43 fmol/mg TE) compared to the controls (323 ± 20.6 fmol/mg TE) ($p < 0.01$). The binding in sections from rats receiving insulin replacement therapy was 384.4 ± 25.1 fmol/mg TE showing 15.97% decrease compared to diabetes group (Figure 2B). Within the hippocampus, diabetic rats exhibited a markedly elevated binding level, specifically 14.4% higher than that observed in the control group (493.1 ± 48.38 fmol/mg TE in diabetic rats versus 430.9 ± 41.3 was significantly higher in the control group) ($p < 0.05$) (Figure 2C). Notably, the insulin replacement group exhibited a 25.16% lower binding level in the hippocampus, with a value of 369.2 ± 15.46 fmol/mg TE, compared to the diabetic group ($p < 0.0001$). In the subcortical

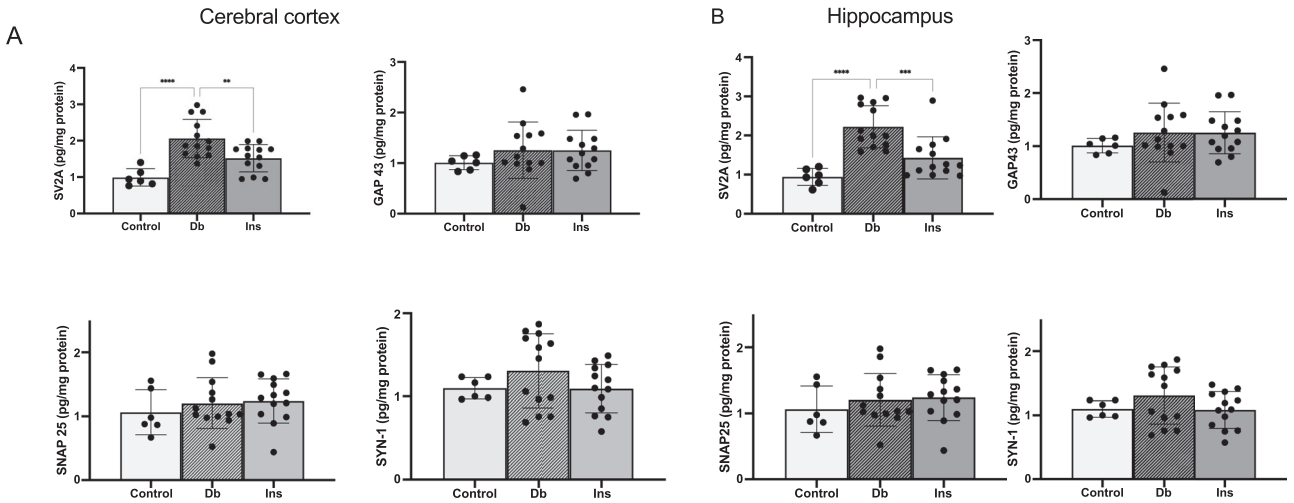

FIGURE 3 | Levels of SV2A, GAP43, SNAP25, and SYN1.
Quantification of presynaptic proteins in extracts from the cerebral cortex (A–D) and the hippocampus (E–H) from control, diabetic (Db), and Insulin-treated (Ins). The synaptic proteins SV2A (A, E), GAP43 (B, F), SNAP25 (C, G), and SYN-1 (D, H) were all measured using ELISA assays and expressed as pg/mg protein. Both in the cerebral cortex and in the hippocampus, the concentration of SV2A was significantly higher in the Db rats compared to the control and Ins groups ($p < 0.0001$). In any of the two tissues, the SV2A concentration in the animals treated with insulin was not different from the control. None of the other proteins displayed a significant difference between the groups. Values were given as mean ± SD. Comparisons were performed between the control, Db, and Ins group for each target protein by one-way ANOVA test. (**$p < 0.01$, *** $p < 0.001$, **** $p < 0.0001$).

structures from the same animals, such as the thalamus and brain stem, there were no differences in [3H]UCB-J binding levels between any of the groups (Figure 2D, E).

3.3 | . Levels of Presynaptic Proteins in the Cerebral Cortex and Hippocampal Tissue

Immunodetection of SV2A using ELISA analysis showed that the concentration of SV2A protein was significantly higher in the cortical homogenates of diabetic rats compared to controls in both the cerebral cortex (Figure 3A) and the hippocampus (Figure 3E).

In the cerebral cortex, SV2A immunoreactivity was significantly increased to 2.1 ± 0.53 pg/mg protein level in diabetic rats, more than double the level observed in controls (0.99 ± 0.24 pg/mg protein) ($p < 0.0001$). The level was significantly and notably reduced to 1.5 ± 0.37 pg/mg protein when the diabetic rats were insulin-treated ($p < 0.01$) (Figure 3A) and was not different from the control. Notably, there were no alterations in other presynaptic proteins, including GAP43, SNAP25, and SYN1, measured in the same cortical extracts across any of the groups (Figure 3B–D).

An identical analysis of hippocampal extracts from the same animals showed similar results. The SV2A concentration in the hippocampus exhibited a more than twofold increase, measuring at 2.2 ± 0.54 pg/mg protein, in contrast to the control level of 0.94 ± 0.21 pg/mg protein ($p < 0.0001$) (Figure 3E). Notably, insulin treatment led to a significant reduction in SV2A protein levels compared to diabetic ($p < 0.001$), but not different from the control. Similarly, among the four synaptic proteins detected, SV2A was the only one that showed a change in the hippocampus of diabetic animals (Figure 3F–H).

3.4 | Gene Expression Levels of all SV2 Paralogues in the Cerebral Cortex and Hippocampus

mRNA levels for the three SV2 family members were analyzed by RT-qPCR and normalized to the housekeeping gene GAPDH (Figure 4). The difference in *Sv2* transcript expression levels was presented as a fold-change relative to the control. *Sv2a* gene expression in the cerebral cortex was 2.1 ± 064-fold higher in diabetic rats than the control rats ($p < 0.001$). Insulin treatment did not restore the *Sv2a* expression, which remained 2.1 ± 0.51-fold higher in the insulin-treated group compared to control ($p < 0.01$) (Figure 4A). *Sv2b* expression showed no changes across any treatment groups (Figure 4B). SV2C expression was significantly higher ($p < 0.0001$) in the diabetic group, measuring 2.9 ± 0.88-fold higher than in the controls. Interestingly, insulin-treated rats showed a 2.1 ± 0.19-fold increase compared to controls, with significant differences from both diabetic ($p < 0.05$) and control rats ($p < 0.01$) (Figure 4C).

Hyperglycemia similarly affected Sv2a and Sv2c expression in the hippocampus, though the effect was less pronounced. *Sv2a* mRNA level was 1.6 ± 0.37-fold higher in diabetic ($p < 0.05$) rats without any significant change in insulin-treated rats (Figure 4D). Hippocampal *Sv2b* expression did not show any change in any of the examined regions including the cortex (Figure 4E). As in the cerebral cortex, the *Sv2c* mRNA level was 1.4 ± 0.32-fold higher in diabetic rats ($p < 0.01$) and 1.33 ± 0.27-fold higher in insulin-treated rats ($p < 0.05$) in the hippocampus (Figure 4F).

3.5 | Correlation Between SV2A Protein, SV2A mRNA, and [3H]UCB-J Binding

Given that SV2A protein concentration and gene expression have been measured by different methods in the same animals, it was

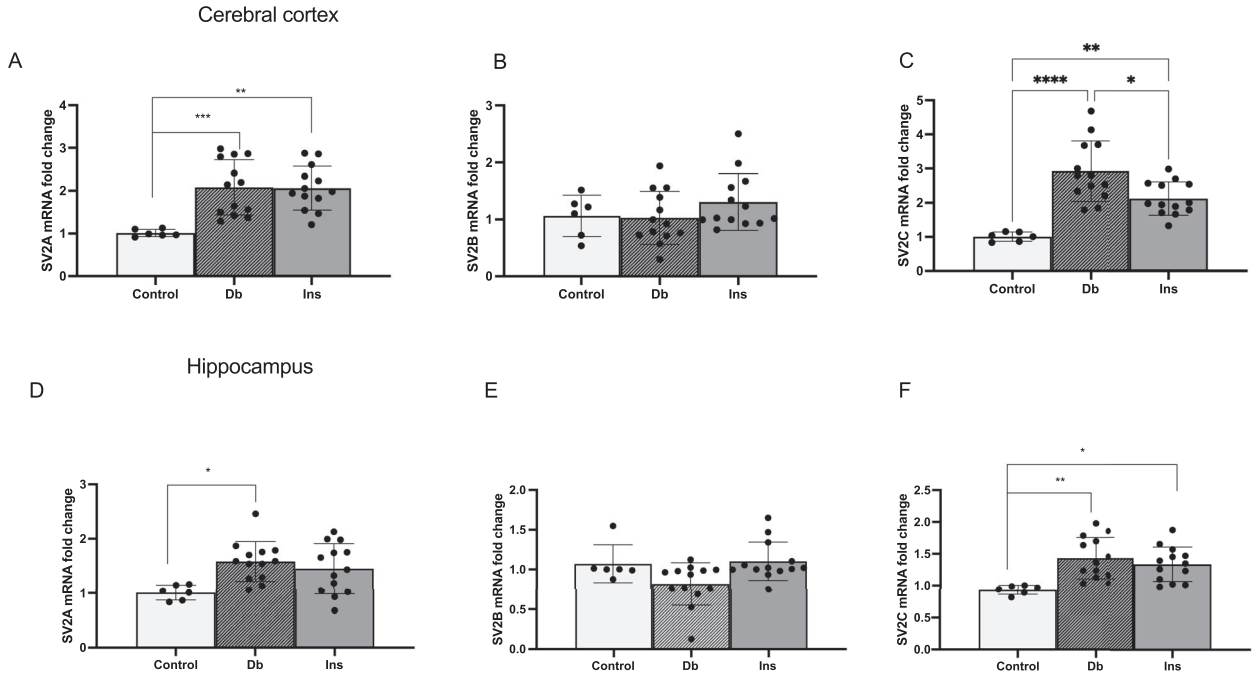

FIGURE 4 | mRNA expression level of *Sv2a, Sv2b*, and *Sv2c*.

RT-qPCR analysis revealed the expression of *Sv2a, Sv2b*, and *Sv2c* in the cerebral cortex (A–C) and the hippocampus (D–F) in Db rats compared to controls, and Ins. The data are expressed as relative fold-change compared to control. The expression levels of both *Sv2a* and *Sv2c* were significantly increased in the diabetic rats compared to the control in both structures, whereas the level of *Sv2b* mRNA was unchanged between groups. Comparisons were performed between the control, Db, and Ins groups for each target gene by one-way ANOVA test. (*$p < 0.05$, **$p < 0.01$, *** $p < 0.001$, **** $p < 0.0001$).

interesting to compare these values across animals. Multiple correlation analysis was conducted among all animals from each of the experimental group. The relationship between S*v2a* transcript level, SV2A protein level (pg/mg), and [^{3}H]UCB-J binding density as a proxy of SV2A protein levels was tested. When conducting a Pearson's correlation analysis, a strong positive and highly significant relationship between SV2A protein levels, as detected by ELISA, and mRNA levels in the cerebral cortex as conducted by RT-qPCR ($r = 0.56$, $p = 0.0009$, $n = 32$) and hippocampal ($r = 0.48$, $p = 0.004$, $n = 32$) homogenates were observed (Figure 5A, B).

″The [3H]UCB-J binding level showed a strong positive correlation with the SV2A protein level in the cerebral cortex ($r = 0.76$; $p < 0.0001$, $n = 20$), but no significant correlation was found in the hippocampus ($r = 0.35$, $p = 0.13$, $n = 20$) (Figure 5C, D).

Neither [^{3}H]UCB-J binding levels in the cerebral cortex ($r = 0.41$, $p = 0.07$) nor in the hippocampus ($r = -0.07$, $p = 0.73$, $n = 20$) showed any correlation with *Sv2a* mRNA levels (data not shown).

3.6 | Glutamate Level of the Cerebral Cortex and Hippocampus

The glutamate levels measured in cortical homogenates increase from 0.036 ± 0.008 nmol/mg protein to 0.070 ± 0.017 nmol/mg after 8 weeks of hyperglycemia ($p < 0.05$). These levels almost returned to baseline (0.054 ± 0.026 nmol/mg protein) in the insulin-treated group. Similarly, hippocampal glutamate levels increased in diabetic rats from 0.036 ± 0.011 nmol/mg protein to 0.064 ± 0.012 nmol/mg protein ($p < 0.05$). Hippocampi from animals treated with insulin exhibited glutamate levels at 0.060 ± 0.028 nmol/mg which was not different from compared to the control ($p < 0.05$) (Figure 6B). Notably, there was a considerable interindividual variability in all groups and especially in the insulin-treated group (Figure 6).

3.7 | Correlation Between SV2A Expression and FBG and Glutamate Levels

Similar to previous correlation analysis, Pearson's correlation coefficient analysis was used to examine any relationship between blood and brain metabolites and SV2A levels.

FBG levels of each rat showed a positive correlation with cortical ($r = 0.66$ $p = 0.0002$, $n = 26$) and hippocampal ($r = 0.68$, $p = 0.0001$, $n = 26$) SV2A protein levels (Figure 7A, B). Similarly, both cortical ($r = 0.65$, $p = 0.05$, $n = 14$) and hippocampal ($r = 0.67$, $p = 0.001$, $n = 14$) [^{3}H]UCB-J binding levels correlated with FBG levels across animals (Figure 7C, D). However, no relationship was found between mRNA levels and FBG levels (data not shown).

A positive correlation between SV2A protein level and glutamate levels was detected in both the cerebral cortex ($r = 0.52$, $p = 0.006$, $n = 26$) and the hippocampus ($r = 0.46$, $p = 0.01$, $n = 26$) (Figure 7E, F). Accordingly, [^{3}H]UCB-J binding levels were also correlated with the glutamate levels of the cerebral cortex ($r = 0.54$, $p = 0.04$, $n = 14$) and hippocampus ($r = 0.63$, $p = 0.02$, $n = 14$) (Figure 7G, H). However, there was no correlation between cortical or hippocampal mRNA levels and glutamate measurements.

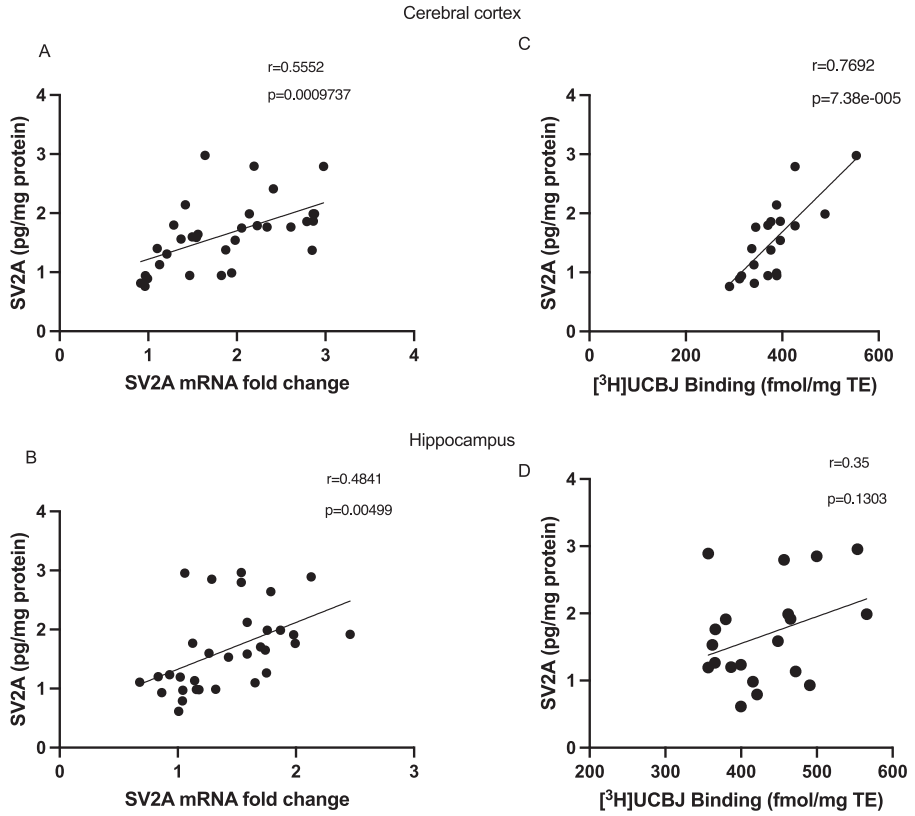

FIGURE 5 | **Correlation of SV2A measures**.
Correlation graphs of SV2A protein (pg/mg protein), *Sv2a* mRNA (A, B), and [^{3}H]UCB-J binding (fmol/mg TE) in cerebral cortex and hippocampus (C, D). Two-tailed Pearson's correlation tests were used to evaluate the linearity between measures. *r* and *p* values were indicated for each graph.

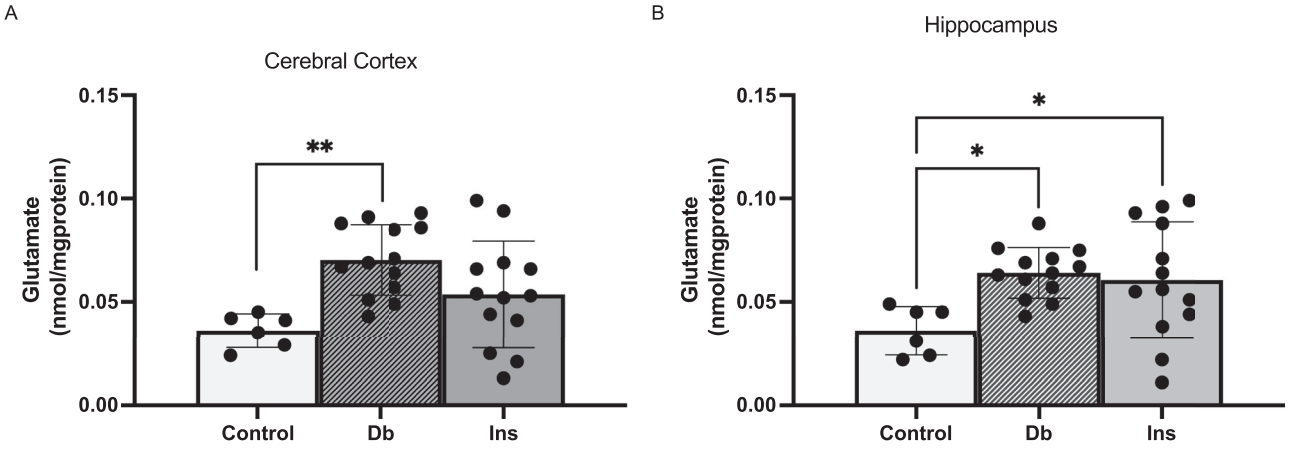

FIGURE 6 | **Glutamate level of cortical and hippocampal homogenates**.
The glutamate level was represented in nmol/mg protein and demonstrated as bargraphs. Glutamate was increased in the cerebral cortex (A) and hippocampus (B) in diabetic rats compared to controls. The level was lower after treatment with insulin, but due to large variability in both groups did not reach significance. Comparisons for glutamate levels were performed between the control, Db, and Ins groups by one-way ANOVA test. Asterisk represents the difference between groups (*$p < 0.05$, **$p < 0.01$).

4 | Discussion

The present study reports that SV2A radioligand binding is significantly increased in the hippocampus and cerebral cortex in male rats after 8 weeks of hyperglycemia. The change is anatomically localized in these structures and not observed in the thalamus and brain stem. The increase in SV2A levels is absent when the diabetic rats were treated with daily insulin, strongly suggesting that the hyperglycemic state is key in regulation of SV2A

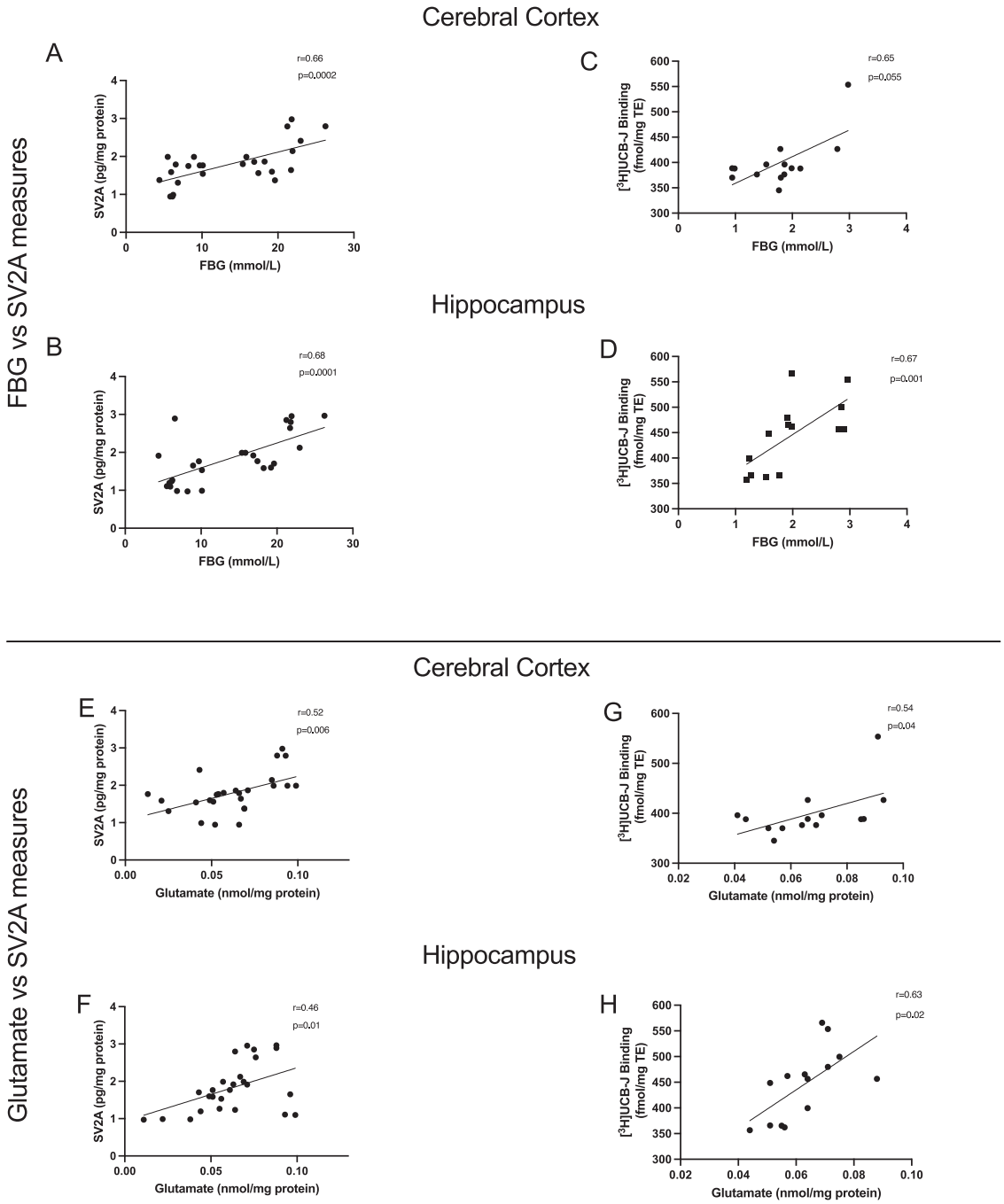

FIGURE 7 | Correlation of FBG and glutamate with SV2A measures in the cerebral cortex and hippocampus.
On the upper part of figure, the correlation between FBG (mmol/L) and SV2A protein (pg/mg protein) (A, B) and [^{3}H]UCB-J binding (fmol/mg TE) (C, D) were shown in both the cerebral cortex and hippocampus. The bottom part shows the correlation between glutamate (nmol/mg protein) and SV2A protein (pg/mg protein) (E, F) and 3H-UCBJ binding (fmol/ mg TE) (G, H) for both the cerebral cortex and hippocampus. Region of interest for correlation graphs were indicated on top of graphs. Two-tailed Pearson's correlation tests were used to evaluate the linearity between measures. *r* and *p* values were indicated for each corresponding graphs.

It is generally accepted that UCB-J binding is a proxy marker for synaptic density (Carson et al. 2022). To confirm this, a direct correlation between binding capacity, the concentration of SV2A, and synaptic numbers in the same tissue would be necessary. Lower levels of binding have previously been interpreted as a marker for synaptic loss (Becker et al. 2020; Carson et al. 2022). However, since these studies compared brains from patients with neurodegenerative conditions, a reduction in SV2A binding may reflect neuronal loss rather than a direct loss of synapses. In the present study, we compared radioligand binding not only with other measures of SV2A expression but also with other well-established biochemical markers of synaptic density (Benowitz et al. 1990; Camporesi et al. 2020; Wang et al. 2023).

We demonstrated a significant increase in binding, most notably in the hippocampus, and to a lesser extent, in the cerebral cortex in diabetic animals. This finding was accompanied by a strong positive correlation to SV2A protein levels, as measured by immune detection in the cerebral cortex. The same positive correlation was found between *Sv2a* mRNA and SV2A protein levels. These data support the validity of each of these measurements. Furthermore, these results strongly suggest that hyperglycemia directly or indirectly induces expression of the *Sv2a* gene leading to increased concentrations of SV2A. Our results indicate that the absence of a correlation between tracer binding and SV2A protein levels in the hippocampus, in contrast to the strong correlation seen in the cerebral cortex. The varying correlations between UCB-J binding and SV2A protein in the hippocampus and cortex imply that there are factors beyond synaptic density that influence binding in a region-specific manner. These factors may include changes in synaptic activity and/or SV2A turnover rates. Collectively our data suggest that SV2A is more than a pure synaptic marker.

To what extent expression of *Sv2a* transcript and protein correlate to binding is more uncertain. A recent study from our laboratory has shown that under steady conditions, mRNA and binding are correlated in the human temporal cortex in the same samples (Pazarlar et al. 2022), but not when comparing different specimens (Johansen et al. 2024). Notably, mRNA and binding in the same neuron are often not present in the same part of the cell, explaining the relatively poor correlation under dynamic conditions such as the hyperglycemic state. Furthermore, our data do not directly support the idea that the rise in SV2A reflects an increase in synaptic density. If that were the case, we would have expected changes not only in SV2A but also in the concentration of other proteins selectively located in the presynapse. However, other established markers of synapse numbers such as GAP43, SNAP25, and SYN-1 (Benowitz et al. 1990; Cai et al. 2024; Camporesi et al. 2020; Wang et al. 2023) did not show alterations in the diabetic animals. This raises concerns about the reliability of SV2A binding as a consistent marker of synapse density, as originally proposed (Finnema et al. 2016; Finnema et al. 2020). Instead, SV2A levels may be selectively influenced by factors unrelated to synaptogenesis or synaptic loss.

Several experimental and clinical studies have investigated the effect of diabetes and hyperglycemia on synaptic plasticity and cognition (Gudala et al. 2013; Gupta et al. 2022; Li et al. 2018; Schernhammer et al. 2011). Experimental studies have shown that chronic diabetic rats or rats exposed to a high-fat diet have impaired cognition (Arnold et al. 2014; Grillo et al. 2019; Stranahan et al. 2009). Genetic diabetic *db/db* mice had a lower number of dendritic spines and hippocampal BDNF levels, and these parameters could be restored by caloric restriction and access to wheel running (Schernhammer et al. 2011). It has also been demonstrated that chronic diabetes leads to changes in both spine density and spine morphology in the cerebral cortex (Joghataie et al. 2007; Martínez-Tellez et al. 2005). Taken together, these findings indicate a potential synaptic decline, and although the aforementioned studies focus on the postsynaptic site, they do not align with the observed higher levels of SV2A.

In relation to SV2A binding in metabolic disease in humans, changes in binding have not been demonstrated in healthy obese individuals, but only in those with concurrent mental conditions. (Asch et al. 2022). Experimentally, no change was seen in the hippocampus and cerebral cortex either in genetically diabetic or obese rats (Kong et al. 2024). However, lower levels of SV2A binding were observed in the prefrontal cortex of minipigs that were given excessive sucrose (Bærentzen et al. 2024). All of these data are based on animal models with higher energy intake and weight gain or models of type II diabetes and obesity, while the current study focuses on extensive pancreas dysfunction and hyperglycemia as a model of type I diabetes.

As SV2A is regulated independently of other presynaptic proteins, it raises the question of what mechanism in the hyperglycemic brain that actually regulates SV2A. Interestingly, the change among synaptic proteins in response to hyperglycemia was specific to only SV2A. This suggests that SV2A is regulated by peripheral hyperglycemia without altering synaptic density or causing structural synaptic remodeling.

Across the animals, we observed a significant positive correlation between FBG levels and UCB-J binding capacity both in the cerebral cortex and hippocampus. Importantly, the reduction of FBG by treatment with insulin also reduced SV2A. Of note, there are structural similarities between SV2A and glucose transporters (Bartholome et al. 2017; Ciruelas et al. 2019), asboth are members of the major facilitator superfamily proteins (Bajjalieh et al. 1992; Bajjalieh et al. 1993; Bajjalieh et al. 1994). Further, SV2A is highly glycosylated and can be modulated by glucose concentration (Madeo et al. 2014). Finally, human SV2A protein expressed in hexose transport deficient yeast cells functions as a galactose transporter, which is inhibited by levetiracetam (Madeo et al. 2014). The regulation of SV2A function by glucose has not been demonstrated in vivo. However, the present data align with brain imaging reports that show a blunt rise in brain glucose under hyperglycemia (Hwang et al. 2017) and that compares UCB-J and FDG PET (Andersen et al. 2023). Other evidence from the clinic also points to a more direct correlation between UCB-J binding and metabolism. Chen et al. (2021) compared the [^{11}C]UCB-J binding and [^{18}F]FDG uptake as a marker of glucose uptake in normal subjects and Alzheimer patients. Notably, [^{18}F]FDG and [^{11}C]UCB-J showed similar patterns of reduction in cortex and hippocampus rather than amyloid load (Chen et al. 2021).

In line with earlier work, elevated glutamate levels were observed in diabetic rats (Bolo et al. 2020; Fried et al. 2019; Roberts et al. 2017; Wiegers et al. 2019). Higher glutamate levels imply increased excitatory neurotransmission, which aligns with other observations showing diabetes-dependent alterations in action potential firing (Roberts et al. 2017), LTP, and alterations in glutamate receptor densities (Valastro et al. 2002). The concentration of glutamate varied considerably between animals, but the variability was reflected by a strong and positive correlation to SV2A levels in both the cerebral cortex and hippocampus. This suggests the intriguing possibility that neuronal activity leads to an increase in SV2A without changes in synaptic density. Supporting evidencecomes from other studies, such as those conducted shortly after status epilepticus (Serrano et al. 2022), where SV2A immunoreactivity is significantly increased under extensive neuronal excitation, before new synapses have had time to form.

In contrast to the expression of *Sv2a*, the other SV2 family member *Sv2b* was not changed. Given the structural homology between different SV2 proteins (Bartholome et al. 2017; Ciruelas et al. 2019), it is believed that they share functions in the presynapse, as the deletion of Sv2a can likely be rescued by the expression of Sv2b (Ciruelas et al. 2019; Crowder et al. 1999).By contrast, only ablation of *Sv2a* and not *Sv2b* causes a reduction in glutamate release (Valastro et al. 2002), and only SV2A-immunoreactive vesicles and not SV2B-positive vesicles are docked in the mouse stratum radiatum synapses (Paulussen et al. 2024). These findings align with our observations, highlighting the distinct regulation of *Sv2a* and *Sv2b*. One could speculate that although SV2A- and SV2B-containing vesicles are morphologically indistinguishable, they may be differentially localized and serve distinct roles in transmitter release (Chanaday and Kavalali 2018). Since *Sv2c* was also upregulated, we might hypothesize a function similar to *Sv2a*; however, its low expression in the brain and restricted distribution make this hypothesis speculative.

Author Contributions

BAP conceived the idea and designed the experiment. CBE and BAP performed the experiments. JDM and BAP interpreted and analyzed the data and EOO provided overall supervision for the project. BAP wrote the first draft. JDM and BAP completed the final draft, and all authors revised the final drafted manuscript.

Acknowledgments

The authors acknowledge and thank UCB Pharma for providing the radioligand for these studies. The project was funded by Izmir Katip Celebi University Scientific Research Project Council with project number 2014-ÖNP-TIPF-0028 to BAP and EOO and the NOVO Nordisk Foundation Tandem Grant (#NNF23OC0081536) to JDM. All experimental data are available upon request from the corresponding authors.

Conflicts of Interest

All authors confirm there is no conflict of interest.

Ethics Statement

All experiments were performed according to the Guide for the Care and Use of Laboratory Animals from the National Institutes of Health Guide for the Care and Use of Laboratory Animals and ARRIVE guidelines. Experiments were approved by the Local Animal Care and Use Committee of Celal Bayar University (Ethical certificate of approval number is 12/11/2014/77.637.435-41).

Data Availability Statement

The data that support the findings of this study are available on request from the corresponding author. The data are not publicly available due to privacy or ethical restrictions.

References

Acharjee, S., B. Ghosh, B. E. Al-Dhubiab, and A. B. Nair. 2013. "Understanding Type 1 Diabetes: Etiology and Models." *Can J Diabetes* 37, no. 4: 269–276. https://doi.org/10.1016/j.jcjd.2013.05.001.

Andersen, K. B., A. K. Hansen, A. C. Schacht, et al. 2023. "Synaptic Density and Glucose Consumption in Patients With Lewy Body Diseases: An [11 C]UCB-J and [18 F]FDG PET Study." *Movement Disorders* 38, no. 5: 796–805. https://doi.org/10.1002/mds.29375.

Arnold, S. E., I. Lucki, B. R. Brookshire, et al. 2014. "High Fat Diet Produces Brain Insulin Resistance, Synaptodendritic Abnormalities and Altered Behavior in Mice." *Neurobiology of Disease* 67: 79–87. https://doi.org/10.1016/j.nbd.2014.03.011.

Asch, R. H., S. E. Holmes, A. M. Jastreboff, et al. 2022. "Lower Synaptic Density Is Associated With Psychiatric and Cognitive Alterations in Obesity." *Neuropsychopharmacology* 47, no. 2: 543–552. https://doi.org/10.1038/s41386-021-01111-5.

Bădescu, S., C. Tătaru, L. Kobylinska, et al. 2016. "The Association Between Diabetes Mellitus and Depression." *Journal of Medicine* 9, no. 2: 120–125.

Bærentzen, S. L., M. B. Thomsen, A. K. Alstrup, et al. 2024. "Excessive Sucrose Consumption Reduces Synaptic Density and Increases Cannabinoid Receptors in Göttingen Minipigs." *Neuropharmacology* 256: 110018. https://doi.org/10.1016/j.neuropharm.2024.110018.

Bajjalieh, S. M., G. D. Frantz, J. M. Weimann, S. K. McConnell, and R. H. Scheller. 1994. "Differential Expression of Synaptic Vesicle Protein 2 (SV2) Isoforms." *Journal of Neuroscience* 14, no. 9: 5223–5235.

Bajjalieh, S. M., K. Peterson, M. Linial, and R. H. Scheller. 1993. "Brain Contains Two Forms of Synaptic Vesicle Protein 2." *PNAS* 90, no. 6: 2150–2154. https://doi.org/10.1073/pnas.90.6.2150.

Bajjalieh, S. M., K. Peterson, R. Shinghal, and R. H. Scheller. 1992. "SV2, a Brain Synaptic Vesicle Protein Homologous to Bacterial Transporters." *Science* 257, no. 5074: 1271–1273. https://doi.org/10.1126/science.1519064.

Bartholome, O., P. Van den Ackerveken, J. Sánchez Gil, et al. 2017. "Puzzling Out Synaptic Vesicle 2 Family Members Functions." *Frontiers in Molecular Neuroscience* 10: 148.

Becker, G., S. Dammicco, M. A. Bahri, and E. Salmon. 2020. "The Rise of Synaptic Density Pet Imaging." *Molecules (Basel, Switzerland)* 25, no. 10: 2303. https://doi.org/10.3390/molecules25102303.

Benowitz, L. I., N. I. Perrone-Bizzozero, R. L. Neve, and W. Rodriguez. 1990. "Chapter 26 GAP-43 as a Marker for Structural Plasticity in the Mature CNS." In *Progress in Brain Research*, edited by PD Coleman, GA Higgins, and CH Phelps. Elsevier, pp 309–320.

Bliss, T. V. P., and G. L. Collingridge. 2013. "Expression of NMDA Receptor-Dependent LTP in the Hippocampus: Bridging the Divide." *Molecular Brain* 6: 5. https://doi.org/10.1186/1756-6606-6-5.

Bluestone, J. A., K. Herold, and G. Eisenbarth. 2010. "Genetics, Pathogenesis and Clinical Interventions in Type 1 Diabetes." *Nature* 464, no. 7293: 1293–1300. https://doi.org/10.1038/nature08933.

Bolo, N. R., A. M. Jacobson, G. Musen, M. S. Keshavan, and D. C. Simonson. 2020. "Acute Hyperglycemia Increases Brain Pregenual Anterior Cingulate Cortex Glutamate Concentrations in Type 1 Diabetes." *Diabetes* 69, no. 7: 1528–1539. https://doi.org/10.2337/db19-0936.

Broadley, M. M., M. J. White, and B. Andrew. 2017. "A Systematic Review and Meta-analysis of Executive Function Performance in Type 1 Diabetes Mellitus." *Psychosomatic medicine* 79, no. 6: 684–696. https://doi.org/10.1097/PSY.0000000000000460.

Cai, H., Y. Pang, Z. Ren, X. Fu, and L. Jia. 2024. "Delivering Synaptic Protein mRNAs via Extracellular Vesicles Ameliorates Cognitive Impairment in a Mouse Model of Alzheimer's Disease." *BMC Medicine* 22: 138. https://doi.org/10.1186/s12916-024-03359-2.

Camporesi, E., J. Nilsson, A. Brinkmalm, et al. 2020. "Fluid Biomarkers for Synaptic Dysfunction and Loss." *Biomark Insights* 15: 1177271920950319. https://doi.org/10.1177/1177271920950319.

Carson, R. E., M. Naganawa, T. Toyonaga, et al. 2022. "Imaging of Synaptic Density in Neurodegenerative Disorders." *Journal of Nuclear Medicine* 63, no. Suppl 1: 60S–67S. https://doi.org/10.2967/jnumed.121.263201.

Chanaday, N. L., and E. T. Kavalali. 2018. "Presynaptic Origins of Distinct Modes of Neurotransmitter Release." *Current Opinion in Neurobiology* 51: 119–126. https://doi.org/10.1016/j.conb.2018.03.005.

Chen, M.-K., A. P. Mecca, M. Naganawa, et al. 2021. "Comparison of [11C]UCB-J and [18F]FDG PET in Alzheimer's Disease: A Tracer Kinetic Modeling Study." *Journal of Cerebral Blood Flow and Metabolism* 41, no. 9: 2395–2409. https://doi.org/10.1177/0271678x211004312.

Ciruelas, K., D. Marcotulli, and S. M. Bajjalieh. 2019. "Synaptic Vesicle Protein 2: A Multi-Faceted Regulator of Secretion." *Seminars in Cell & Developmental Biology* 95: 130–141. https://doi.org/10.1016/j.semcdb.2019.02.003.

Crowder, K. M., J. M. Gunther, T. A. Jones, et al. 1999. "Abnormal Neurotransmission in Mice Lacking Synaptic Vesicle Protein 2A (SV2A)." *PNAS* 96, no. 26: 15268–15273. https://doi.org/10.1073/pnas.96.26.15268.

d'Almeida, O. C., I. R. Violante, B. Quendera, C. Moreno, L. Gomes, and M. Castelo-Branco. 2020. "The Neurometabolic Profiles of GABA and Glutamate as Revealed by Proton Magnetic Resonance Spectroscopy in Type 1 and Type 2 Diabetes." *PLoS ONE* 15, no. 10: e0240907. https://doi.org/10.1371/journal.pone.0240907.

Deeds, M. C., J. M. Anderson, A. S. Armstrong, et al. 2011. "Single Dose Streptozotocin-Induced Diabetes: Considerations for Study Design in Islet Transplantation Models." *Laboratory Animals* 45, no. 3: 131–140. https://doi.org/10.1258/la.2010.010090.

Ding, X., C. Fang, X. Li, et al. 2019. "Type 1 diabetes-associated cognitive impairment and diabetic peripheral neuropathy in Chinese adults: results from a prospective cross-sectional study." *BMC endocrine disorders* 19, no. 1: 34. https://doi.org/10.1186/s12902-019-0359-2.

Dorsemans, A.-C., D. Couret, A. Hoarau, O. Meilhac, C. Lefebvre d'Hellencourt, and N. Diotel. 2017. "Diabetes, Adult Neurogenesis and Brain Remodeling: New Insights From Rodent and Zebrafish Models." *Neurogenesis (Austin)* 4, no. 1: e1281862. https://doi.org/10.1080/23262133.2017.1281862.

Finnema, S. J., N. B. Nabulsi, T. Eid, et al. 2016. "Imaging Synaptic Density in the Living Human Brain." *Science Translational Medicine* 8, no. 348: 348ra96. https://doi.org/10.1126/scitranslmed.aaf6667.

Finnema, S. J., T. Toyonaga, K. Detyniecki, et al. 2020. "Reduced Synaptic Vesicle Protein 2A Binding in Temporal Lobe Epilepsy: A [11C]UCB-J Positron Emission Tomography Study." *Epilepsia* 61, no. 10: 2183–2193. https://doi.org/10.1111/epi.16653.

Fried, P. J., A. Pascual-Leone, and N. R. Bolo. 2019. "Diabetes and the Link Between Neuroplasticity and Glutamate in the Aging Human Motor Cortex." *Clinical Neurophysiology* 130, no. 9: 1502–1510. https://doi.org/10.1016/j.clinph.2019.04.721.

Furman, B. L. 2015. "Streptozotocin-Induced Diabetic Models in Mice and Rats." *Current Protocols in Pharmacology* 70: 5.47.1–5.47.20. https://doi.org/10.1002/0471141755.ph0547s70.

Grillo, C. A., J. L. Woodruff, V. A. Macht, and L. P. Reagan. 2019. "Insulin Resistance and Hippocampal Dysfunction: Disentangling Peripheral and Brain Causes From Consequences." *Experimental Neurology* 318: 71–77. https://doi.org/10.1016/j.expneurol.2019.04.012.

Gudala, K., D. Bansal, F. Schifano, and A. Bhansali. 2013. "Diabetes Mellitus and Risk of Dementia: A Meta-Analysis of Prospective Observational Studies." *Journal of Diabetes Investigation* 4, no. 6: 640–650. https://doi.org/10.1111/jdi.12087.

Gupta, M., S. Pandey, M. Rumman, B. Singh, and A. A. Mahdi. 2022. "Molecular Mechanisms Underlying Hyperglycemia Associated Cognitive Decline." *IBRO Neuroscience Reports* 14: 57–63. https://doi.org/10.1016/j.ibneur.2022.12.006.

Hiremath, S. B., A. A. Gautam, P. J. George, A. Thomas, R. Thomas, and G. Benjamin. 2019. "Hyperglycemia-Induced Seizures—Understanding the Clinico- Radiological Association." *Indian Journal of Radiology and Imaging* 29, no. 4: 343–349. https://doi.org/10.4103/ijri.IJRI_344_19.

Hwang, J. J., L. Jiang, M. Hamza, et al. 2017. "Blunted Rise in Brain Glucose Levels During Hyperglycemia in Adults With Obesity and T2DM." *JCI Insight* 2, no. 20: e95913. https://doi.org/10.1172/jci.insight.95913.

Janz, R., Y. Goda, M. Geppert, M. Missler, and T. C. Südhof. 1999. "SV2A and SV2B Function as Redundant Ca2+ Regulators in Neurotransmitter Release." *Neuron* 24, no. 4: 1003–1016. https://doi.org/10.1016/s0896-6273(00)81046-6.

Joghataie, M.-T., M. Roghani, M.-R. Jalali, T. Baluchnejadmojarad, and M. Sharayeli. 2007. "Dendritic Spine Changes in Medial Prefrontal Cortex of Male Diabetic Rats Using Golgi-Impregnation Method." *Archives of Iranian Medicine* 10, no. 1: 54–58.

Johansen, A., V. Beliveau, E. Colliander, et al. 2024. "An in Vivo High-Resolution human Brain Atlas of Synaptic Density." *Journal of Neuroscience* 44, no. 33: e1750232024. https://doi.org/10.1523/JNEUROSCI.1750-23.2024.

Kong, Y., L. Cao, F. Xie, et al. 2024. "Reduced SV2A and GABAA Receptor Levels in the Brains of Type 2 Diabetic Rats Revealed by [18F]SDM-8 and [18F]Flumazenil PET." *Biomedicine & Pharmacotherapy* 172: 116252. https://doi.org/10.1016/j.biopha.2024.116252.

Last, D., D. C. Alsop, A. M. Abduljalil, et al. 2007. "Global and Regional Effects of Type 2 Diabetes on Brain Tissue Volumes and Cerebral Vasoreactivity." *Diabetes Care* 30, no. 5: 1193–1199. https://doi.org/10.2337/dc06-2052.

Li, W., G. Roy Choudhury, A. Winters, et al. 2018. "Hyperglycemia Alters Astrocyte Metabolism and Inhibits Astrocyte Proliferation." *Aging and Disease* 9, no. 4: 674–684. https://doi.org/10.14336/AD.2017.1208.

Lynch, B. A., N. Lambeng, K. Nocka, et al. 2004. "The Synaptic Vesicle Protein SV2A Is the Binding Site for the Antiepileptic Drug Levetiracetam." *PNAS* 101, no. 26: 9861–9866. https://doi.org/10.1073/pnas.0308208101.

Madeo, M., A. D. Kovács, and D. A. Pearce. 2014. "The human Synaptic Vesicle Protein, SV2A, Functions as a Galactose Transporter in Saccharomyces Cerevisiae." *Journal of Biological Chemistry* 289, no. 48: 33066–33071. https://doi.org/10.1074/jbc.C114.584516.

Martínez-Tellez, R., M. de Jesús Gómez-Villalobos, and G. Flores. 2005. "Alteration in Dendritic Morphology of Cortical Neurons in Rats With Diabetes Mellitus Induced by Streptozotocin." *Brain Research* 1048, no. 1–2: 108–115. https://doi.org/10.1016/j.brainres.2005.04.048.

Menten-Dedoyart, C., M. E. Serrano Navacerrada, O. Bartholome, et al. 2016. "Development and Validation of a New Mouse Model to Investigate the Role of sv2a in Epilepsy." *PLoS ONE* 11, no. 11: e0166525. https://doi.org/10.1371/journal.pone.0166525.

Michiels, L., A. Delva, J. van Aalst, et al. 2021. "Synaptic Density in Healthy human Aging Is Not Influenced by Age or Sex: A 11C-UCB-J PET Study." *Neuroimage* 232: 117877. https://doi.org/10.1016/j.neuroimage.2021.117877.

Nissen, T. D., T. Meldgaard, R. W. Nedergaard, et al. 2020. "Peripheral, Synaptic and central Neuronal Transmission Is Affected in Type 1 Diabetes." *Journal of Diabetes and Its Complications* 34, no. 9: 107614. https://doi.org/10.1016/j.jdiacomp.2020.107614.

Okamoto, M. M., G. F. Anhê, R. Sabino-Silva, et al. 2011. "Intensive Insulin Treatment Induces Insulin Resistance in Diabetic Rats by Impairing Glucose Metabolism-Related Mechanisms in Muscle and Liver." *Journal of Endocrinology* 211, no. 1: 55–64. https://doi.org/10.1530/JOE-11-0105.

Pan, A., M. Lucas, Q. Sun, et al. 2010. "Bidirectional Association Between Depression and Type 2 Diabetes Mellitus in Women." *Archives of Internal Medicine* 170, no. 21: 1884–1891. https://doi.org/10.1001/archinternmed.2010.356.

Paulussen, I., H. Beckert, T. F. Musial, et al. 2024. "SV2B Defines a Subpopulation of Synaptic Vesicles." *Journal of Molecular Cell Biology* 15, no. 9: mjad054. https://doi.org/10.1093/jmcb/mjad054.

Pazarlar, B. A., S. S. Aripaka, V. Petukhov, L. Pinborg, K. Khodosevich, and J. D. Mikkelsen. 2022. "Expression Profile of Synaptic Vesicle Glycoprotein 2A, B, and C Paralogues in Temporal Neocortex Tissue From Patients With Temporal Lobe Epilepsy (TLE)." *Molecular Brain* 15, no. 1: 45. https://doi.org/10.1186/s13041-022-00931-w.

Pfaffl, M. W. 2001. “A New Mathematical Model for Relative Quantification in Real-Time RT-PCR.” *Nucleic Acids Research* 29, no. 9: e45. https://doi.org/10.1093/nar/29.9.e45.

Roberts, B. L., M. Zhu, H. Zhao, C. Dillon, and S. M. Appleyard. 2017. “High Glucose Increases Action Potential Firing of Catecholamine Neurons in the Nucleus of the Solitary Tract by Increasing Spontaneous Glutamate Inputs.” *American Journal of Physiology. Regulatory, Integrative and Comparative Physiology* 313, no. 3: R229–R239. https://doi.org/10.1152/ajpregu.00413.2016.

Rocha, D. S., M. V. Dentz, J. F. A. Model, et al. 2022. “Female Wistar Rats Present Particular Glucose Flux When Submitted to Classic Protocols of Experimental Diabetes.” *Biomedical Journal* 46, no. 3: 100539. https://doi.org/10.1016/j.bj.2022.05.004.

Rossano, S., T. Toyonaga, S. J. Finnema, et al. 2020. “Assessment of a White Matter Reference Region for ^{11}C-UCB-J PET Quantification.” *Journal of Cerebral Blood Flow and Metabolism* 40, no. 9: 1890–1901. https://doi.org/10.1177/0271678x19879230.

Schernhammer, E., J. Hansen, K. Rugbjerg, L. Wermuth, and B. Ritz. 2011. “Diabetes and the Risk of Developing parkinson’s Disease in denmark.” *Diabetes Care* 34, no. 5: 1102–1108. https://doi.org/10.2337/dc10-1333.

Serrano, M. E., E. Kim, M. M. Petrinovic, F. Turkheimer, and D. Cash. 2022. “Imaging Synaptic Density: The Next Holy Grail of Neuroscience?” *Frontiers in Neuroscience* 16: 796129.

Stafstrom, C. E. 2003. “Hyperglycemia Lowers Seizure Threshold.” *Epilepsy Currents* 3, no. 4: 148–149. https://doi.org/10.1046/j.1535-7597.2003.03415.x.

Stranahan, A. M., K. Lee, B. Martin, et al. 2009. “Voluntary Exercise and Caloric Restriction Enhance Hippocampal Dendritic Spine Density and BDNF Levels in Diabetic Mice.” *Hippocampus* 19, no. 10: 951–961. https://doi.org/10.1002/hipo.20577.

Tan, A. M., O. A. Samad, T. Z. Fischer, P. Zhao, A.-K. Persson, and S. G. Waxman. 2012. “Maladaptive Dendritic Spine Remodeling Contributes to Diabetic Neuropathic Pain.” *The Journal of Neuroscience* 32, no. 20: 6795. https://doi.org/10.1523/JNEUROSCI.1017-12.2012.

Terpstra, M., A. Moheet, A. Kumar, L. E. Eberly, E. Seaquist, and G. Öz. 2014. “Changes in human Brain Glutamate Concentration During Hypoglycemia: Insights Into Cerebral Adaptations in Hypoglycemia-Associated Autonomic Failure in Type 1 Diabetes.” *Journal of Cerebral Blood Flow and Metabolism* 34, no. 5: 876–882. https://doi.org/10.1038/jcbfm.2014.32.

Valastro, B., J. Cossette, N. Lavoie, S. Gagnon, F. Trudeau, and G. Massicotte. 2002. “Up-regulation of Glutamate Receptors Is Associated With LTP Defects in the Early Stages of Diabetes Mellitus.” *Diabetologia* 45, no. 5: 642–650. https://doi.org/10.1007/s00125-002-0818-5.

Wang, Q., S. Tao, L. Xing, et al. 2023. “SNAP25 is a Potential Target for Early Stage Alzheimer’s Disease and Parkinson’s Disease.” *European Journal of Medical Research* 28: 570. https://doi.org/10.1186/s40001-023-01360-8.

Wiegers, E. C., H. M. Rooijackers, J. J. A. van Asten, et al. 2019. “Elevated Brain Glutamate Levels in Type 1 Diabetes: Correlations With Glycaemic Control and Age of Disease Onset but Not With Hypoglycaemia Awareness Status.” *Diabetologia* 62, no. 6: 1065–1073. https://doi.org/10.1007/s00125-019-4862-9.

Zhao, F., J. Li, L. Mo, et al. 2016. “Changes in Neurons and Synapses in Hippocampus of Streptozotocin-Induced Type 1 Diabetes Rats: A Stereological Investigation.” *Anat Rec (Hoboken)* 299, no. 9: 1174–1183. https://doi.org/10.1002/ar.23344.